

## Supporting Information

### ADA'DA small molecule acceptors with non-fully-fused core units

Xiujuan Chen,<sup>‡ab</sup> Yue Luo,<sup>‡bc</sup> Menglan Lv,<sup>d</sup> Chenyi Yi,<sup>e</sup> Meizhen Yin,<sup>\*a</sup> Shengjian Liu,<sup>\*c</sup> Zuo Xiao<sup>\*b</sup> and Liming Ding<sup>\*b</sup>

<sup>a</sup> School of Materials Science and Engineering, Beijing University of Chemical Technology, Beijing 100029, China. E-mail: yinmz@mail.buct.edu.cn

<sup>b</sup> Center for Excellence in Nanoscience (CAS), Key Laboratory of Nanosystem and Hierarchical Fabrication (CAS), National Center for Nanoscience and Technology, Beijing 100190, China. E-mail: xiaoz@nanoctr.cn, ding@nanoctr.cn

<sup>c</sup> School of Chemistry, South China Normal University, Guangzhou 510006, China. E-mail: shengjian.liu@m.scnu.edu.cn

<sup>d</sup> School of Chemistry and Chemical Engineering, Guizhou University, Guiyang 550025, China.

<sup>e</sup> Department of Electrical Engineering, Tsinghua University, Beijing 100084, China.

<sup>‡</sup> X. Chen and Y. Luo contributed equally to this work.

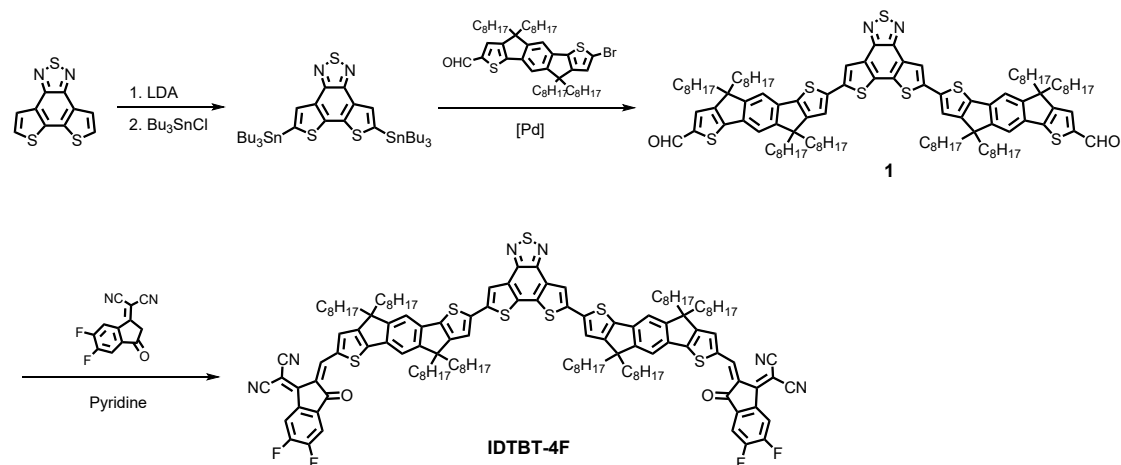
\* Corresponding authors.

## 1. General characterization

$^1\text{H}$  and  $^{13}\text{C}$  NMR spectra were measured on a Bruker Avance-400 spectrometer. Absorption spectra were recorded on a Shimadzu UV-1800 spectrophotometer. Cyclic voltammetry was done by using a Shanghai Chenhua CHI620D voltammetric analyzer under argon in an anhydrous acetonitrile solution of tetra-*n*-butylammonium hexafluorophosphate (0.1 M). A glassy-carbon electrode was used as the working electrode, a platinum-wire was used as the counter electrode, and a Ag/Ag<sup>+</sup> electrode was used as the reference electrode. IDTBT-4F and IDTP-4F were coated onto glassy-carbon electrode and all potentials were corrected against Fc/Fc<sup>+</sup>. AFM was performed on a Multimode microscope (Veeco) by using tapping mode. TEM was performed on a Hitachi HT7700 transmission electron microscope at an accelerating voltage of 100.0 kV.

## 2. Synthesis

All reagents were purchased from J&K Co., Aladdin Co., Innochem Co., Derthon Co., SunaTech Co. and other commercial suppliers. 7-Bromo-4,4,9,9-tetraoctyl-4,9-dihydro-*s*-indaceno[1,2-*b*:5,6-*b'*]dithiophene-2-carbaldehyde<sup>[1]</sup> and L1-S<sup>[2]</sup> were synthesized according to literature. All reactions dealing with air- or moisture-sensitive compounds were carried out by using standard Schlenk techniques.



**Scheme 1** Synthesis of IDTBT-4F.

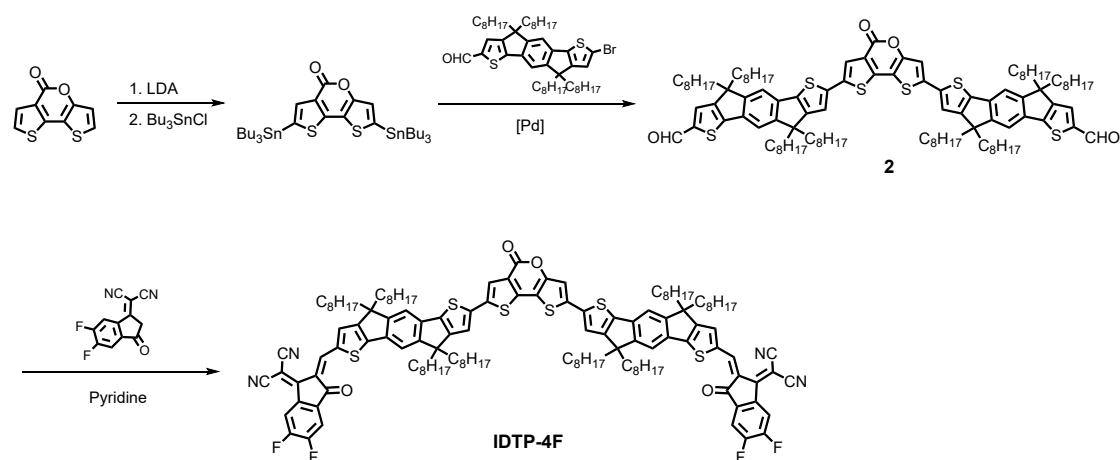
### 5,8-Bis(tributylstannyl)dithieno[3',2':3,4;2'',3'':5,6]benzo[1,2-*c*][1,2,5]thiadiazole.

To a solution of dithieno[3',2':3,4;2'',3'':5,6]benzo[1,2-*c*][1,2,5]thiadiazole (1 g, 4.0 mmol) in THF (100 mL) was added LDA (20.1 mmol) at -40 °C. The mixture was stirred -40 °C for 1 h. To the mixture was added Bu<sub>3</sub>SnCl (4.4 mL, 16.1 mmol). The mixture was stirred at 0 °C for 1 h. The mixture was poured into water and extracted with CH<sub>2</sub>Cl<sub>2</sub>. The solution passed through a alkaline Al<sub>2</sub>O<sub>3</sub> column with petroleum ether:CH<sub>2</sub>Cl<sub>2</sub> (2:1) as eluent to give crude 5,8-

bis(tributylstannyl)dithieno[3',2':3,4;2'',3'':5,6]benzo[1,2-c][1,2,5]thiadiazole as a yellow oil (2.15 g, 65%). The resulting ditin reagent was not further purified and was directly used for the next step.

**Compound 1.** To a solution of 7-bromo-4,4,9,9-tetraoctyl-4,9-dihydro-s-indaceno[1,2-b:5,6-b']dithiophene-2-carbaldehyde (353 mg, 0.43 mmol) and 5,8-bis(tributylstannyl)dithieno[3',2':3,4;2'',3'':5,6]benzo[1,2-c][1,2,5]thiadiazole (141.9 mg, 0.17 mmol) in toluene (10 mL) and DMF (2 mL) was added Pd(PPh<sub>3</sub>)<sub>4</sub> (19.8 mg, 0.02 mmol) under N<sub>2</sub>. The mixture was heated to reflux and stirred overnight. After removal of the solvent, the product was purified via column chromatography (silica gel) by using petroleum ether:CH<sub>2</sub>Cl<sub>2</sub> (1:2) as eluent to give compound 1 as a red oil (164 mg, 55%). <sup>1</sup>H NMR (CDCl<sub>3</sub>, 400 MHz, δ/ppm): 9.91 (s, 2H), 8.15 (s, 2H), 7.64 (s, 2H), 7.44 (s, 2H), 7.36 (s, 2H), 7.29 (s, 2H), 2.09-1.88 (m, 16H), 1.25-1.14 (m, 80H), 0.88-0.79 (m, 40H). <sup>13</sup>C NMR (CDCl<sub>3</sub>, 100 MHz, δ/ppm): 182.88, 157.22, 155.31, 155.16, 153.66, 152.32, 150.38, 144.75, 141.89, 138.88, 138.30, 137.81, 134.51, 133.34, 130.52, 129.78, 119.77, 119.20, 114.86, 113.48, 54.43, 54.16, 39.03, 31.80, 29.97, 29.94, 29.30, 29.24, 29.21, 24.30, 24.26, 22.62, 14.08. MALDI-TOF MS (m/z): C<sub>46</sub>H<sub>60</sub>N<sub>2</sub>S<sub>3</sub> (M<sup>+</sup>) calc. 1729.96, found 1729.47.

**IDTBT-4F.** To a solution of compound 1 (164 mg, 0.09 mmol) and DFIC (109 mg, 0.5 mmol) in CHCl<sub>3</sub> (16 mL) and pyridine (0.6 mL) was heated at 65 °C for 2 h. The mixture was purified via column chromatography (silica gel) by using CHCl<sub>3</sub> as eluent. IDTBT-4F was obtained as a dark blue solid (160 mg, 78%). <sup>1</sup>H NMR (CDCl<sub>3</sub>, 400 MHz, δ/ppm): 8.95 (s, 2H), 8.56-8.52 (m, 2H), 8.17 (br, 2H), 7.72 (s, 2H), 7.69-7.65 (m, 2H), 7.59 (s, 2H), 7.38 (br, 2H), 7.32 (br, 2H), 2.12-1.93 (m, 16H), 1.22-1.14 (m, 80H), 0.88-0.80 (m, 40H). <sup>13</sup>C NMR (CDCl<sub>3</sub>, 100 MHz, δ/ppm): 185.95, 163.82, 158.61, 157.02, 155.51, 153.03, 152.89, 150.32, 140.24, 138.59, 136.50, 134.50, 133.47, 129.93, 119.76, 114.98, 114.77, 114.64, 113.61, 112.47, 112.30, 68.17, 54.41, 54.28, 39.15, 38.95, 31.79, 31.77, 29.96, 29.89, 29.29, 29.23, 29.20, 24.38, 24.31, 22.61, 22.59, 14.06. MALDI-TOF MS (m/z): C<sub>46</sub>H<sub>60</sub>N<sub>2</sub>S<sub>3</sub> (M<sup>+</sup>) calc. 2153.999, found 2154.521.



**Scheme 2** Synthesis of IDTP-4F.

**2,7-Bis(tributylstannyl)-5H-dithieno[3,2-b:2',3'-d]pyran-5-one.** To a solution of 5H-dithieno[3,2-b:2',3'-d]pyran-5-one (500 mg, 2.4 mmol) in THF (50 mL) was added LDA (12.0 mmol) at -40 °C. The mixture was stirred -40 °C for 1 h. To the mixture was added Bu<sub>3</sub>SnCl (2.6 mL, 9.6 mmol). The mixture was stirred at 0 °C for 1 h. The mixture was poured into water and extracted with CH<sub>2</sub>Cl<sub>2</sub>. The solution passed through an alkaline Al<sub>2</sub>O<sub>3</sub> column with petroleum ether:CH<sub>2</sub>Cl<sub>2</sub> (2:1) as eluent to give crude 2,7-bis(tributylstannyl)-5H-dithieno[3,2-b:2',3'-d]pyran-5-one as a yellow oil (1.11 g, 53%). The resulting ditin reagent was not further purified and was directly used for the next step.

**Compound 2.** To a solution of 7-bromo-4,4,9,9-tetraoctyl-4,9-dihydro-s-indaceno[1,2-b:5,6-b']dithiophene-2-carbaldehyde (279 mg, 0.34 mmol) and 2,7-bis(tributylstannyl)-5H-dithieno[3,2-b:2',3'-d]pyran-5-one (107 mg, 0.14 mmol) in toluene (5 mL) and DMF (1 mL) was added Pd(PPh<sub>3</sub>)<sub>4</sub> (15.7 mg, 0.01 mmol) under N<sub>2</sub>. The mixture was heated to reflux and stirred overnight. After removal of the solvent, the product was purified via column chromatography (silica gel) by using petroleum ether:CH<sub>2</sub>Cl<sub>2</sub> (2:1) as eluent to give compound 2 as a red oil (207 mg, 90%). <sup>1</sup>H NMR (CDCl<sub>3</sub>, 400 MHz, δ/ppm): 9.90 (s, 2H), 7.70 (br, 1H), 7.63 (s, 2H), 7.43 (s, 2H), 7.33 (s, 2H), 7.21 (br, 1H), 7.19 (br, 1H), 7.15 (br, 1H), 2.07-1.90 (m, 16H), 1.25-1.12 (m, 80H), 0.88-0.79 (m, 40H). <sup>13</sup>C NMR (CDCl<sub>3</sub>, 100 MHz, δ/ppm): 182.86, 157.20, 157.05, 155.41, 155.14, 153.66, 152.80, 152.19, 144.90, 143.02, 138.48, 138.18, 137.79, 136.55, 134.87, 130.45, 129.27, 126.00, 122.46, 121.15, 119.69, 114.85, 113.53, 112.66, 54.46, 54.39, 54.13, 38.97, 31.77, 29.90, 29.69, 29.26, 29.19, 29.17, 24.26, 24.20, 22.59, 14.06. MALDI-TOF MS (m/z): C<sub>46</sub>H<sub>60</sub>N<sub>2</sub>S<sub>3</sub> (M<sup>+</sup>) calc. 1689.97, found 1689.47.

**IDTP-4F.** To a solution of compound 2 (207 mg, 0.12 mmol) and DFIC (141 mg, 0.6 mmol) in CHCl<sub>3</sub> (21 mL) and pyridine (0.8 mL) was heated at 65 °C for 2 h. The mixture was purified via column chromatography (silica gel) by using CHCl<sub>3</sub> as eluent. Then methanol was added and the resulting mixture was filtered to give IDTP-4F as a dark blue solid (163 mg, 63%). <sup>1</sup>H NMR (CDCl<sub>3</sub>, 400 MHz, δ/ppm): 8.96 (s, 2H), 8.57-8.53 (m, 2H), 7.72-7.66 (m, 5H), 7.58 (s, 2H), 7.35 (br, 2H), 7.22 (br, 3H), 2.07-1.91 (m, 16H), 1.24-1.14 (s, 80H), 0.97-0.79 (m, 40H). <sup>13</sup>C NMR (CDCl<sub>3</sub>, 100 MHz, δ/ppm): 185.97, 163.67, 158.68, 158.50, 158.41, 156.94, 155.66, 153.05, 152.90, 139.50, 138.64, 136.49, 134.47, 119.72, 115.00, 114.79, 114.60, 113.73, 113.02, 112.52, 112.33, 68.38, 68.27, 54.46, 54.27, 39.11, 38.90, 31.77, 31.76, 29.91, 29.86, 29.26, 29.20, 29.18, 24.35, 24.27, 22.60, 22.58, 14.06. MALDI-TOF MS (m/z): C<sub>46</sub>H<sub>60</sub>N<sub>2</sub>S<sub>3</sub> (M<sup>+</sup>) calc. 2114.011, found 2114.543.

### 3. NMR

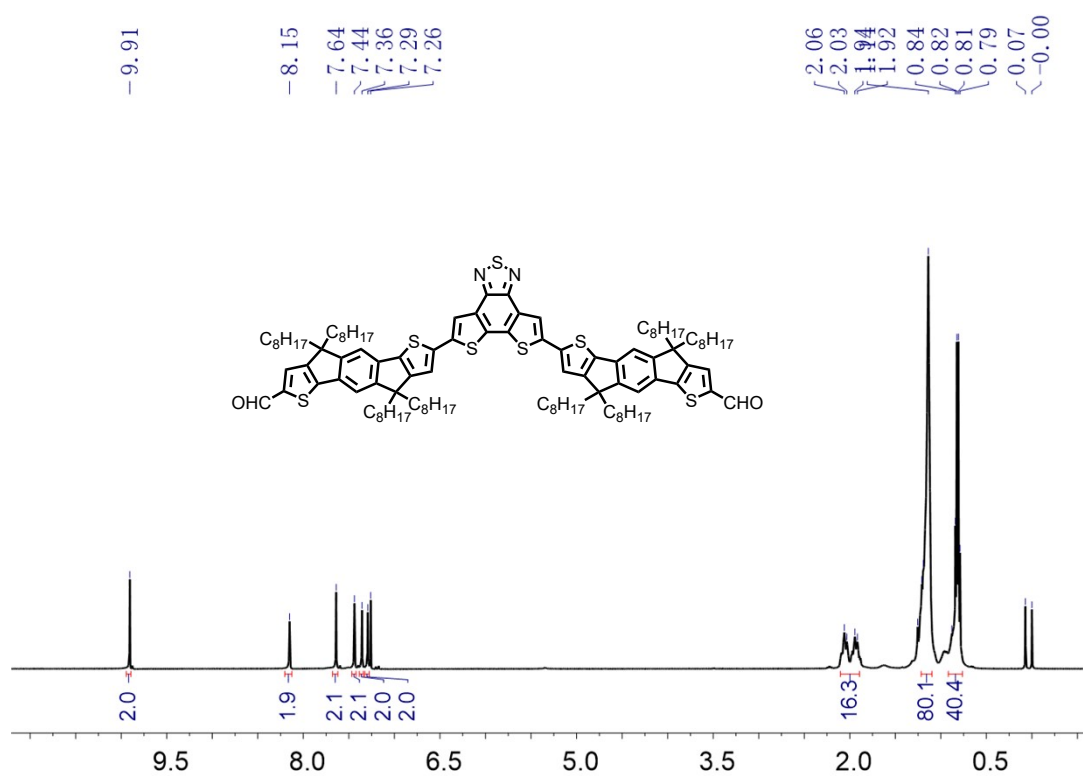


**Fig. S1** <sup>1</sup>H NMR spectrum of **compound 1**.

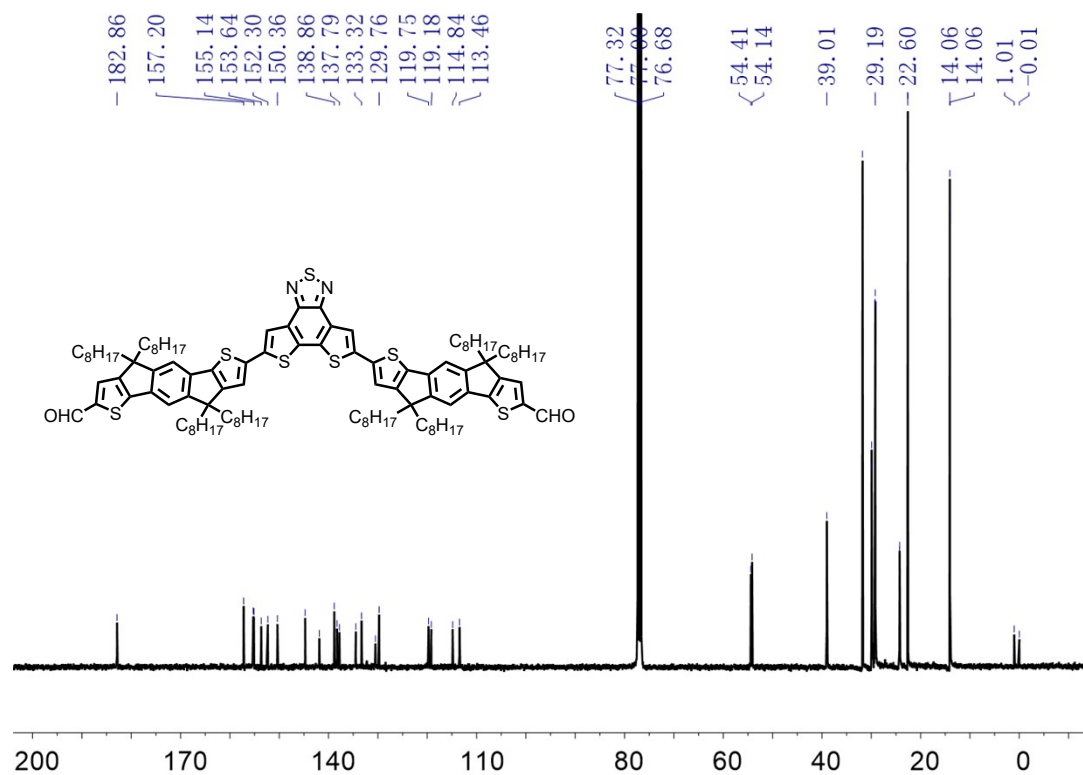


**Fig. S2** <sup>13</sup>C NMR spectrum of **compound 1**.

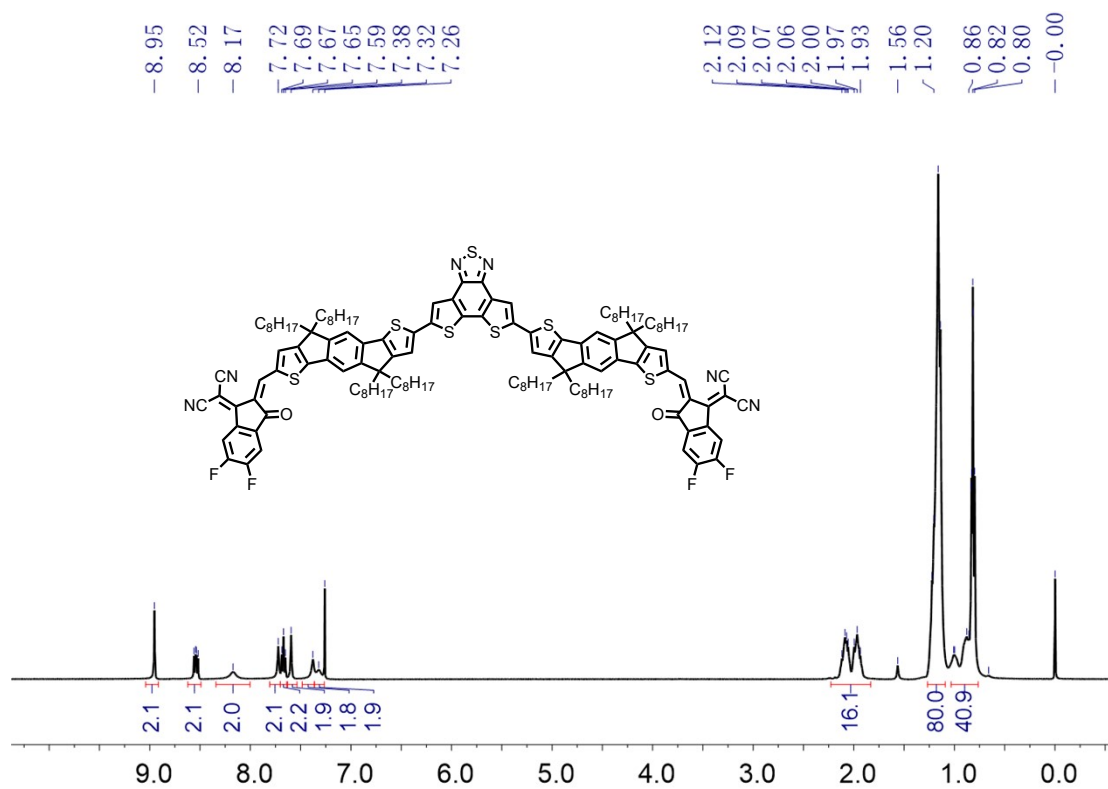


Fig. S3  $^1\text{H}$  NMR spectrum of IDTBT-4F.

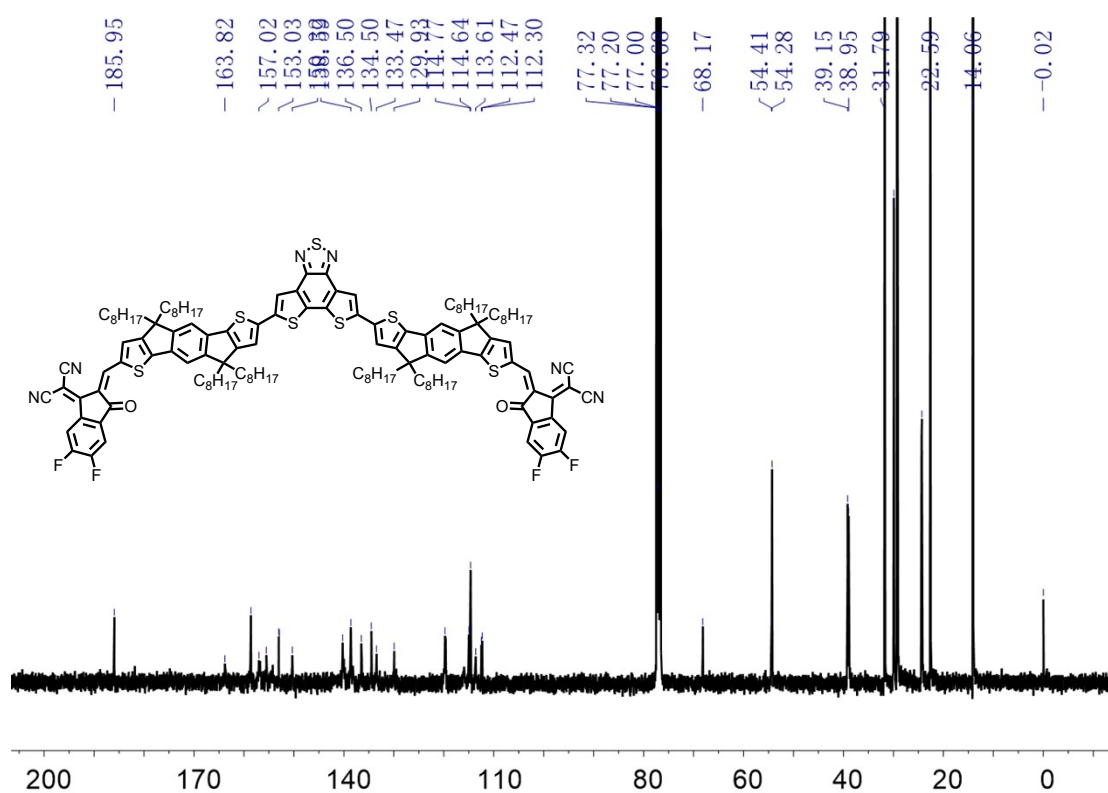


Fig. S4  $^{13}\text{C}$  NMR spectrum of IDTBT-4F.

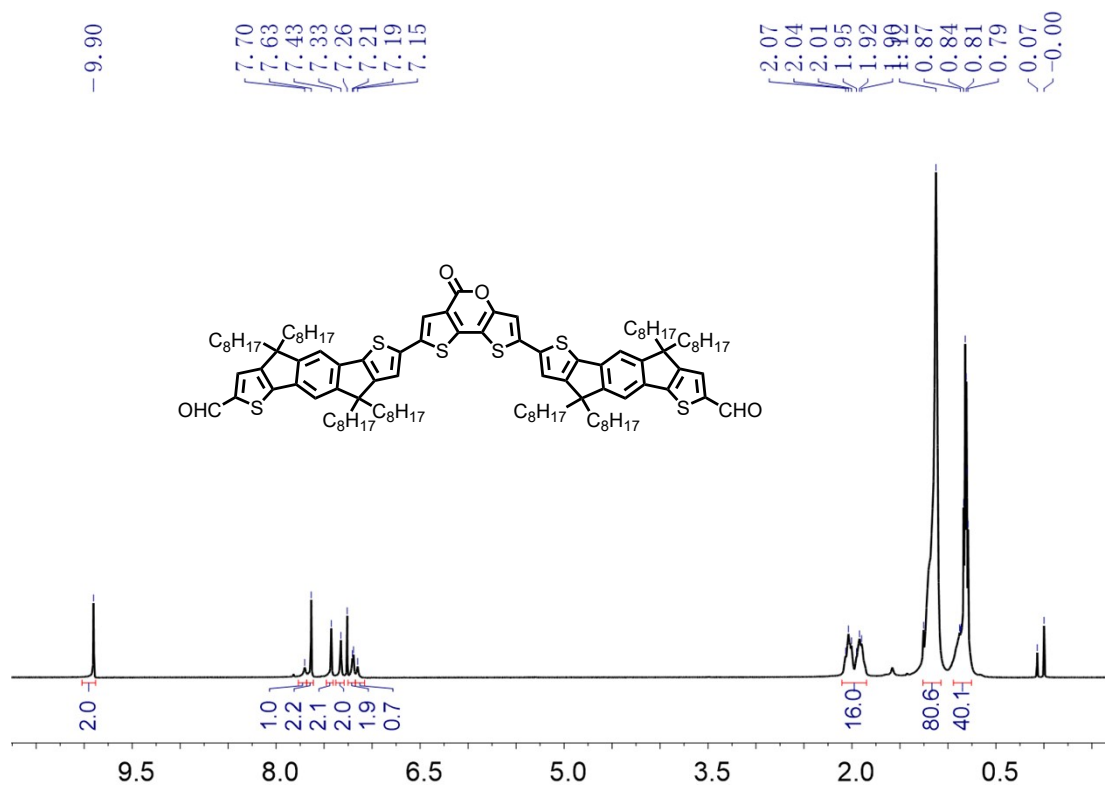


Fig. S5  $^1\text{H}$  NMR spectrum of compound 2.

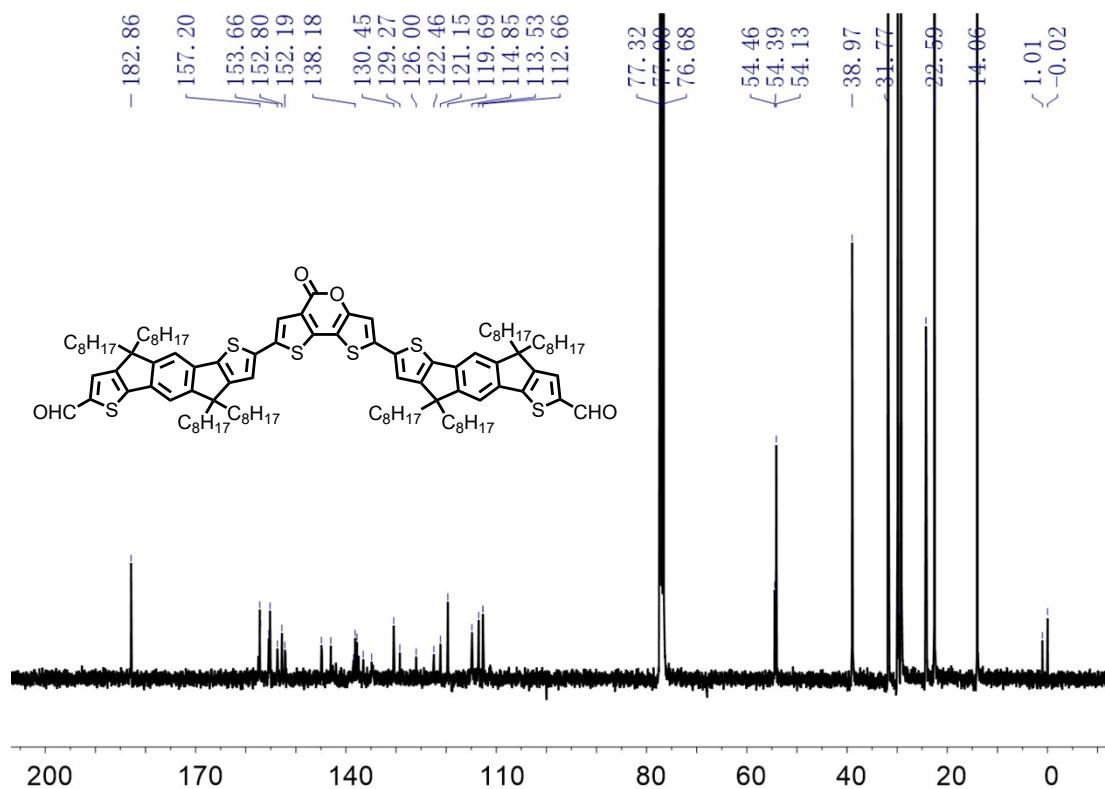


Fig. S6  $^{13}\text{C}$  NMR spectrum of compound 2.

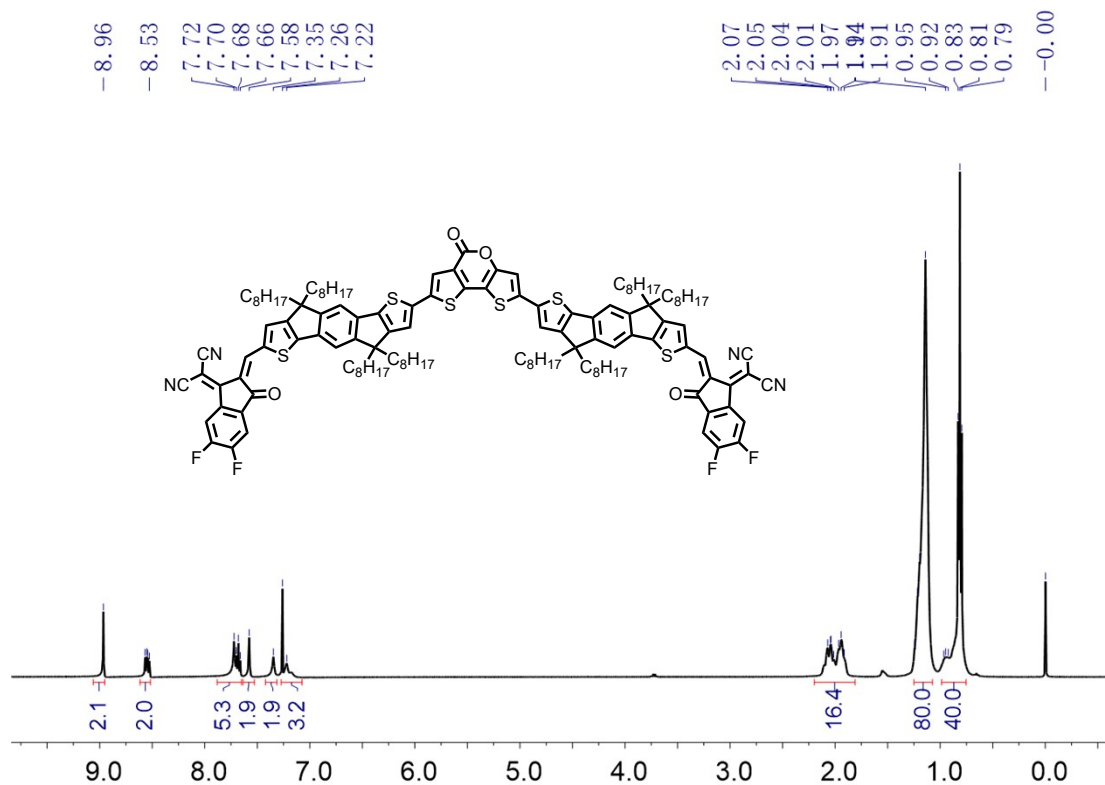


Fig. S7  $^1\text{H}$  NMR spectrum of IDTP-4F.

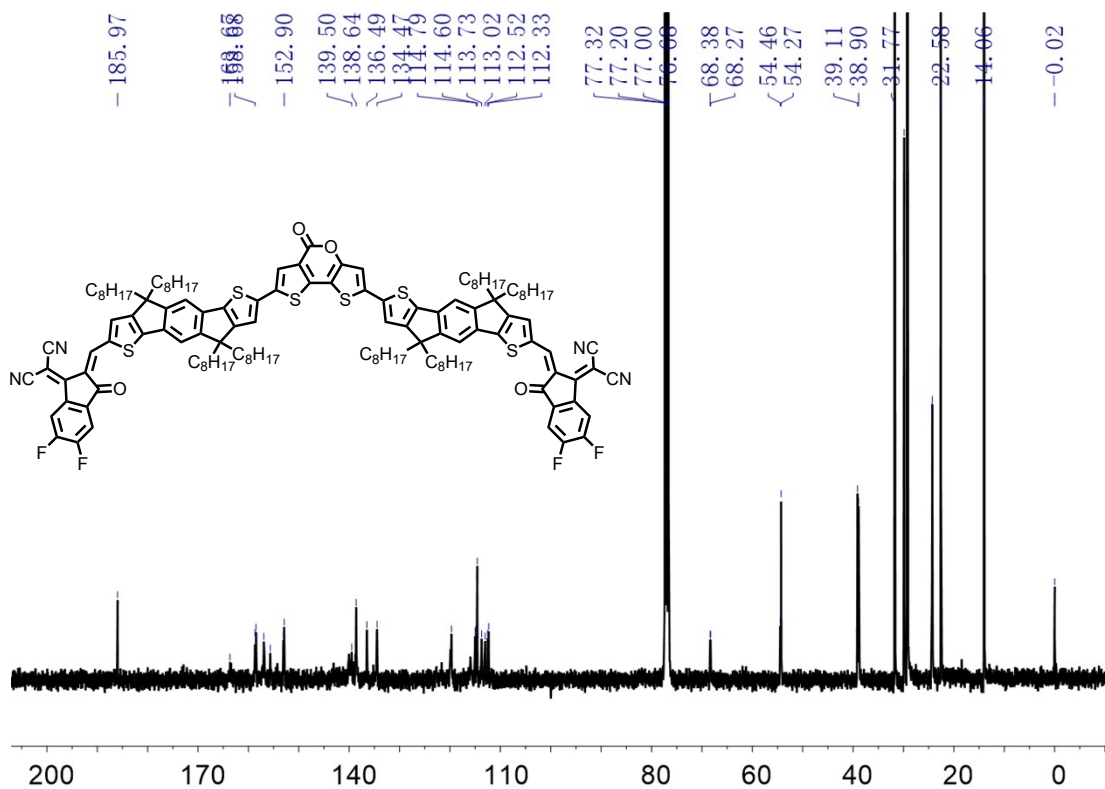
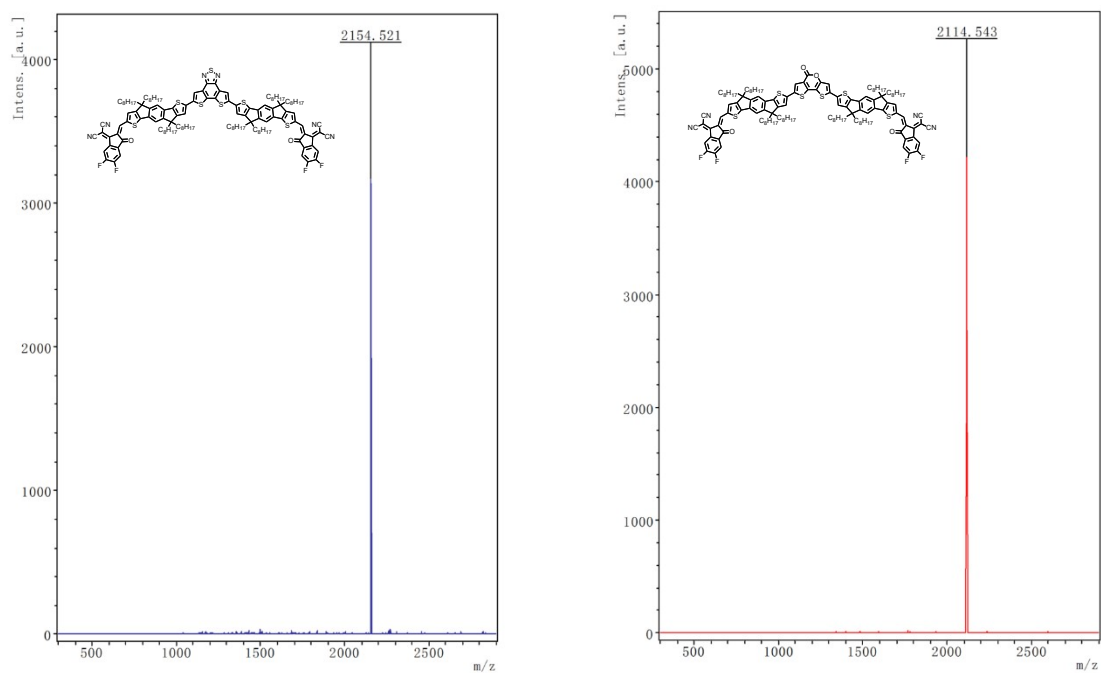


Fig. S8  $^{13}\text{C}$  NMR spectrum of IDTP-4F.

#### 4. Mass spectra for IDTBT-4F and IDTP-4F





**Fig. S9** MALDI-TOF mass spectra for IDTBT-4F and IDTP-4F.

## 5. CV

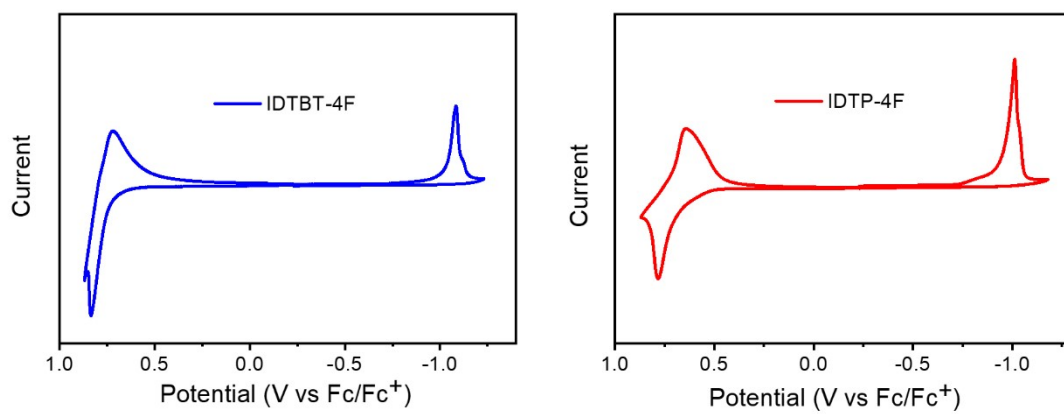


**Fig. S10** Cyclic voltammograms for IDTBT-4F and IDTP-4F.

## 6. DFT

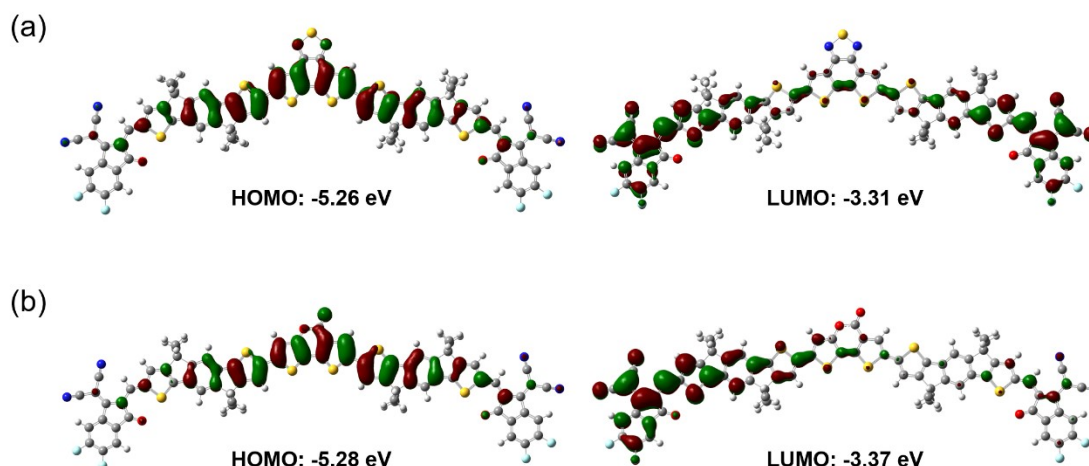


Fig. S11 DFT-predicted HOMO and LUMO for (a) IDTBT-4F and (b) IDTP-4F.

## 7. Device fabrication and measurements

### Conventional solar cells

A 30 nm thick PEDOT:PSS layer was made by spin-coating an aqueous dispersion onto ITO glass (4000 rpm for 30 s). PEDOT:PSS substrates were dried at 150 °C for 15 min. A L1-S:IDTBT-4F (or L1-S:IDTP-4F) blend in chloroform (CF) was spin-coated onto PEDOT:PSS. PDIN (2 mg/mL) in MeOH:AcOH (1000:3) was spin-coated onto active layer (5000 rpm for 30 s). Ag (~80 nm) was evaporated onto PDIN through a shadow mask (pressure ca.  $10^{-4}$  Pa). The effective area for the devices is 4 mm<sup>2</sup>. The thicknesses of the active layers were measured by using a KLA Tencor D-120 profilometer. *J-V* curves were measured by using a computerized Keithley 2400 SourceMeter and a Xenon-lamp-based solar simulator (Enli Tech, AM 1.5G, 100 mW/cm<sup>2</sup>). The illumination intensity of solar simulator was determined by using a monocrystalline silicon solar cell (Enli SRC2020, 2cm×2cm) calibrated by NIM. The external quantum efficiency (EQE) spectra were measured by using a QE-R3011 measurement system (Enli Tech).

### Electron-only devices

The structure for electron-only devices is ITO/ZnO/acceptor/PDIN/Al. The ZnO precursor sol-gel was obtained from stirring the solution of 1.0 g Zn(CH<sub>3</sub>COO)<sub>2</sub>·2H<sub>2</sub>O in 10 mL ethylene glycol monomethyl ether and 275 μL ethylenediamine. The ZnO films were prepared by spin-coating the ZnO precursor onto the UV-ozone-treated ITO substrates and then thermally annealing at 200 °C for 20 min in atmosphere. A IDTBT-4F (or IDTP-4F) CF solution was spin-coated onto ZnO. PDIN (2 mg/mL) was spin-coated onto acceptor (5000 rpm for 30 s). Finally, Al (~100 nm) was successively evaporated onto the PDIN through a shadow mask (pressure ca.  $10^{-4}$  Pa). *J-V* curves were measured by using a computerized Keithley 2400 SourceMeter in the dark.

## 8. SCLC

Charge carrier mobility was measured by SCLC method. The mobility was determined by fitting the dark current to the model of a single carrier SCLC, which is described by:

$$J = \frac{9}{8} \varepsilon_0 \varepsilon_r \mu \frac{V^2}{d^3}$$

where  $J$  is the current density,  $\mu$  is the zero-field mobility of electrons,  $\varepsilon_0$  is the permittivity of the vacuum,  $\varepsilon_r$  is the relative permittivity of the material,  $d$  is the thickness of the blend film, and  $V$  is the effective voltage ( $V = V_{\text{appl}} - V_{\text{bi}}$ , where  $V_{\text{appl}}$  is the applied voltage, and  $V_{\text{bi}}$  is the built-in potential determined by electrode work function difference). Here,  $V_{\text{bi}} = 0$  V for electron-only devices.<sup>[3]</sup> The mobility was calculated from the slope of  $J^{1/2}$ - $V$  plot.

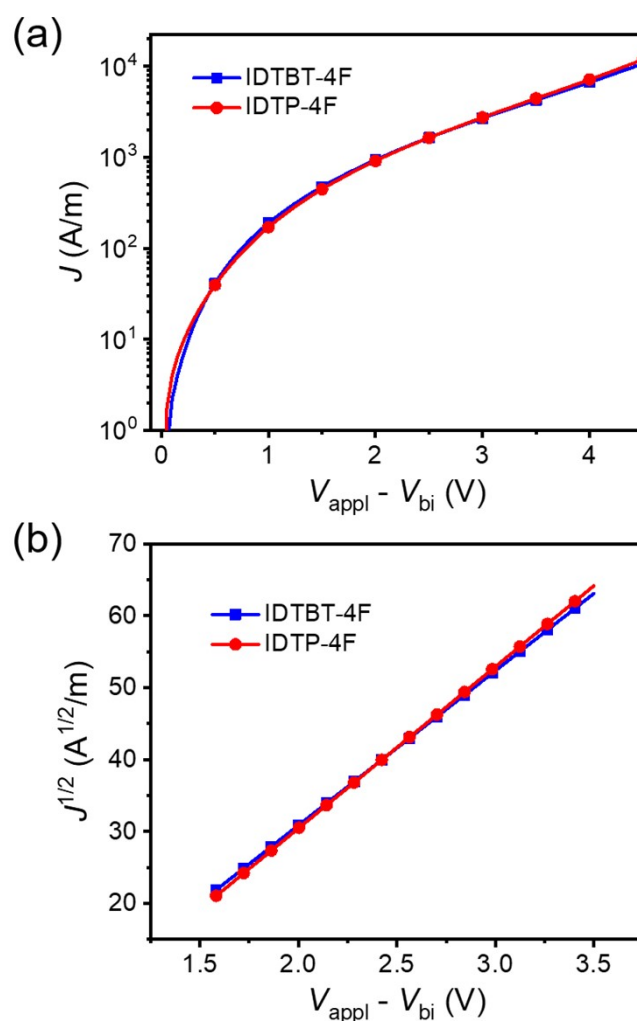


**Fig. S12**  $J$ - $V$  curve (a) and corresponding  $J^{1/2}$ - $V$  plot (b) for the electron-only devices (in dark). The thicknesses for IDTBT-4F and IDTP-4F films are 127 nm and 129 nm, respectively.

## 9. Optimization of device performance

**Table S1** Optimization of D/A ratio for L1-S:IDTBT-4F conventional solar cells.<sup>a</sup>

D/A [w/w]	$V_{oc}$ [V]	$J_{sc}$ [mA/cm <sup>2</sup> ]	FF [%]	PCE [%]
1:0.6	0.956	17.43	65.77	10.96 (10.54) <sup>b</sup>
1:1	0.974	18.09	68.10	12.00 (11.78)
1:1.4	0.985	16.09	69.80	11.06 (10.98)
1:1.8	0.984	14.41	67.13	9.51 (9.48)

<sup>a</sup>Blend solution: 13 mg/mL in CF; spin-coating: 4000 rpm for 30 s.

<sup>b</sup>Data in parentheses are averages for 8 cells.

**Table S2** Optimization of active layer thickness for L1-S:IDTBT-4F conventional solar cells.<sup>a</sup>

Thickness [nm]	$V_{oc}$ [V]	$J_{sc}$ [mA/cm <sup>2</sup> ]	FF [%]	PCE [%]
142	0.960	16.55	63.62	10.11 (10.00) <sup>b</sup>
120	0.968	17.34	66.76	11.20 (11.17)
102	0.974	18.09	68.10	12.00 (11.90)
88	0.975	16.93	68.23	11.27 (11.23)
76	0.976	16.51	69.11	11.14 (11.10)

<sup>a</sup>D/A ratio: 1:1 (w/w); blend solution: 13 mg/mL in CF.

<sup>b</sup>Data in parentheses are averages for 8 cells.

**Table S3** Optimization of DIO content for L1-S:IDTBT-4F conventional solar cells.<sup>a</sup>

DIO [vol%]	$V_{oc}$ [V]	$J_{sc}$ [mA/cm <sup>2</sup> ]	FF [%]	PCE [%]
0	0.974	18.09	68.10	12.00 (11.90) <sup>b</sup>
0.1	0.981	17.02	67.76	11.32 (11.20)
0.3	0.964	17.51	66.01	11.14 (11.10)
0.5	0.979	16.67	62.10	10.13 (10.09)

<sup>a</sup>D/A ratio: 1:1 (w/w); blend solution: 13 mg/mL in CF; spin-coating: 4000 rpm for 30 s.

<sup>b</sup>Data in parentheses stand are averages for 8 cells.

**Table S4** Optimization of D/A ratio for L1-S:IDTP-4F conventional solar cells.<sup>a</sup>

D/A [w/w]	$V_{oc}$ [V]	$J_{sc}$ [mA/cm <sup>2</sup> ]	FF [%]	PCE [%]
1:0.6	0.943	17.10	58.48	9.43 (9.32) <sup>b</sup>
1:1	0.953	18.03	65.24	11.21 (11.18)
1:1.4	0.968	16.33	69.55	11.00 (10.95)
1:1.8	0.980	14.90	69.45	10.15 (10.07)

<sup>a</sup>Blend solution: 12.5 mg/mL in CF; spin-coating: 4000 rpm for 30 s.

<sup>b</sup>Data in parentheses are averages for 8 cells.

**Table S5** Optimization of active layer thickness for L1-S:IDTP-4F conventional solar cells.<sup>a</sup>

Thickness [nm]	$V_{oc}$ [V]	$J_{sc}$ [mA/cm <sup>2</sup> ]	FF [%]	PCE [%]
143	0.943	16.32	62.10	9.56 (9.48) <sup>b</sup>
118	0.946	17.43	64.80	10.69 (10.60)
99	0.953	18.03	65.24	11.21 (11.18)
86	0.949	17.34	66.33	10.91 (10.90)
75	0.952	16.70	67.69	10.76 (10.62)

<sup>a</sup>D/A ratio: 1:1 (w/w); blend solution: 12.5 mg/mL in CF.

<sup>b</sup>Data in parentheses are averages for 8 cells.

**Table S6** Optimization of DIO content for L1-S:IDTP-4F conventional solar cells.<sup>a</sup>

DIO [vol%]	$V_{oc}$ [V]	$J_{sc}$ [mA/cm <sup>2</sup> ]	FF [%]	PCE [%]
0	0.953	18.03	65.24	11.21 (11.18) <sup>b</sup>
0.1	0.959	17.70	67.95	11.53 (11.49)
0.3	0.945	18.49	68.23	11.92 (11.82)
0.5	0.942	17.01	59.62	9.55 (9.39)

<sup>a</sup>D/A ratio: 1:1 (w/w); blend solution: 12.5 mg/mL in CF; spin-coating: 4000 rpm for 30 s.

<sup>b</sup>Data in parentheses stand are averages for 8 cells.

## 10. Exciton dissociation probability

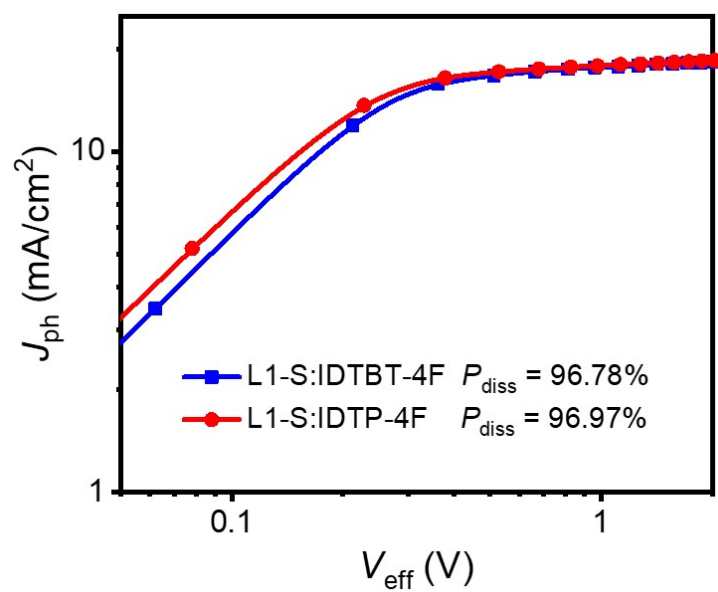


Fig. S13  $J_{ph}$ - $V_{eff}$  plot.

## 11. Bimolecular recombination

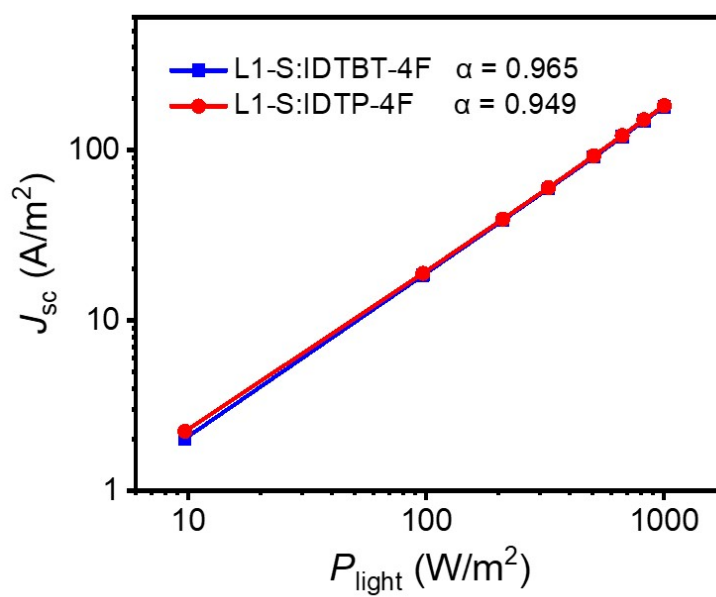
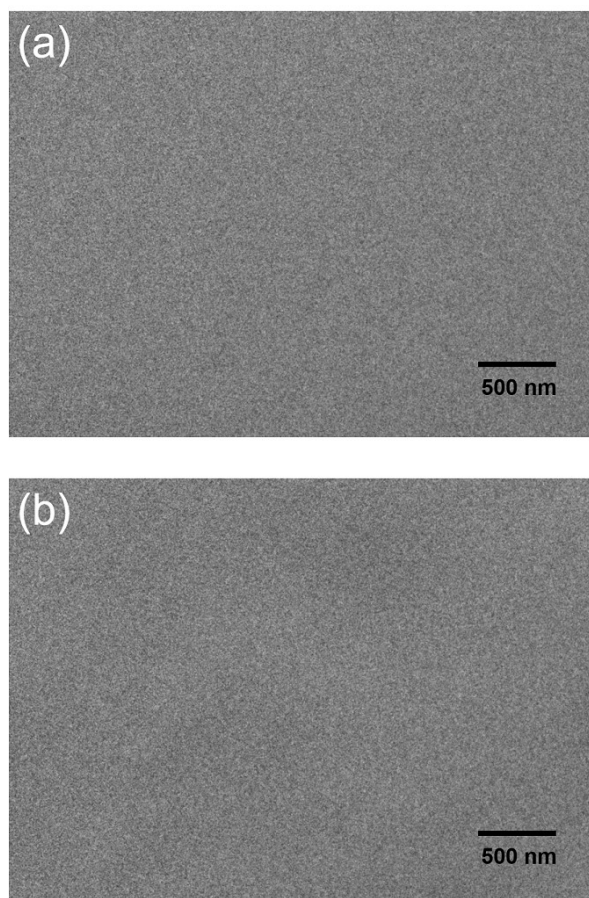


Fig. S14  $J_{sc}$ - $P_{light}$  plots.

## 12. TEM



**Fig. S15** TEM images for (a) L1-S:IDTBT-4F and (b) L1-S:IDTP-4F blend films.

## References

- [1] H. S. Kim, S. Rasool, W. S. Shin, C. E. Song and D.-H. Hwang, Alkylated Indacenodithiophene-Based Non-fullerene Acceptors with Extended  $\pi$ -Conjugation for High-Performance Large-Area Organic Solar Cells, *ACS Appl. Mater. Interfaces*, 2020, **12**, 50638.
- [2] Y. Jiang, K. Jin, X. Chen, Z. Xiao, X. Zhang and L. Ding, Post-sulphuration enhances the performance of a lactone polymer donor, *J. Semicond.*, 2021, **42**, 070501.
- [3] C. Duan, W. Cai, B. B. Y. Hsu, C. Zhong, K. Zhang, C. Liu, Z. Hu, F. Huang, G. C. Bazan, A. J. Heeger and Y. Cao, Toward green solvent processable photovoltaic materials for polymer solar cells: the role of highly polar pendant groups in charge carrier transport and photovoltaic behavior, *Energy Environ. Sci.*, 2013, **6**, 3022.